

# New Phytologist

**Nitrogen demand, availability, and acquisition strategy control plant responses to elevated CO<sub>2</sub> at different scales**

Journal:	<i>New Phytologist</i>
Manuscript ID	NPH-MS-2024-46044
Manuscript Type:	Full Paper
Date Submitted by the Author:	19-Jan-2024
Complete List of Authors:	Perkowski, Evan; Texas Tech University, Dept. of Biological Sciences Ezekannagha, Ezinwanne; Texas Tech University, Dept. of Biological Sciences Smith, Nicholas; Texas Tech University, Dept. of Biological Sciences
Key Words:	acclimation, eco-evolutionary optimality, growth chamber, least-cost theory, nitrogen acquisition strategy, photosynthesis, plant functional ecology, whole-plant growth

SCHOLARONE™  
Manuscripts

1   **"Nitrogen demand, availability, and acquisition strategy control plant responses to elevated  
2   CO<sub>2</sub> at different scales"**

3

4   Evan A. Perkowski<sup>1,\*</sup>, Ezinwanne Ezekannagha<sup>1</sup>, Nicholas G. Smith<sup>1</sup>

5   <sup>1</sup>Department of Biological Sciences, Texas Tech University, Lubbock, TX

6

7   \*Corresponding author:

8   2901 Main St.

9   Lubbock, TX, 79409

10   Email: [evan.a.perkowski@ttu.edu](mailto:evan.a.perkowski@ttu.edu)

11

12   **ORCIDs:** Evan A. Perkowski (0000-0002-9523-8892), Ezinwanne Ezekannagha (0000-0001-  
13   7469-949X), Nicholas G. Smith (0000-0001-7048-4387)

14

15   Total word count: 6436

16        -   Introduction: 1298

17        -   Methods: 2369

18        -   Results: 1027

19        -   Discussion: 1742

20

21   Tables: 3

22   Figures: 3

23   Supporting Information: 6 tables, 6 figures

24      **Summary**

- 25      • Plants respond to elevated atmospheric CO<sub>2</sub> concentrations (eCO<sub>2</sub>) by reducing  
26      photosynthetic capacity, a response that corresponds with increased net photosynthesis,  
27      primary productivity, and growth. These responses are commonly assumed to be  
28      constrained by nitrogen availability. However, recent work using eco-evolutionary  
29      optimality theory suggests that nitrogen demand for building and maintaining  
30      photosynthetic enzymes, which optimizes resource allocation to photosynthetic capacity  
31      and maximizes allocation to growth, may be a stronger driver of plant responses to eCO<sub>2</sub>.  
32      • Here, we examined leaf physiological and whole-plant growth responses of *Glycine max*  
33      L. (Merr) seedlings subjected to full-factorial combinations of two CO<sub>2</sub>, two inoculation,  
34      and nine nitrogen fertilization treatments.  
35      • Nitrogen fertilization and inoculation did not modify leaf photosynthetic responses to  
36      eCO<sub>2</sub>. Instead, eCO<sub>2</sub> downregulated the maximum rate of Rubisco carboxylation more  
37      strongly than it decreased the maximum rate of electron transport for RuBP regeneration,  
38      increasing net photosynthesis rates by approaching optimal coordination. Increasing  
39      fertilization enhanced positive whole-plant responses to eCO<sub>2</sub> due to increased nitrogen  
40      uptake and reduced nitrogen acquisition costs.  
41      • Patterns expected from eco-evolutionary optimality theory determined leaf  
42      photosynthetic responses to eCO<sub>2</sub>, while nitrogen availability constrained whole-plant  
43      responses. Results suggest that nitrogen availability and demand each drive plant  
44      responses to eCO<sub>2</sub>, though operate at different scales

45

46      **Plain Language Summary**

47      Plant responses to elevated CO<sub>2</sub> are commonly assumed to be regulated by nitrogen availability.  
48      However, recent work suggests that demand for building and maintaining photosynthetic  
49      enzymes may be a stronger predictor of plant responses to elevated CO<sub>2</sub>. Here, we reconcile  
50      these competing ideas, showing that nitrogen demand determines leaf responses while nitrogen  
51      availability controls whole-plant responses to elevated CO<sub>2</sub>.

52

53      **Keywords**

54 acclimation, eco-evolutionary optimality, growth chamber, least-cost theory, nitrogen acquisition  
55 strategy, photosynthesis, plant functional ecology, whole-plant growth

56

57 **Introduction**

58 Complex carbon and nitrogen cycles regulate terrestrial ecosystems. Terrestrial biosphere  
59 models, which are beginning to include coupled carbon and nitrogen cycles (Davies-Barnard *et*  
60 *al.*, 2020; Kou-Giesbrecht *et al.*, 2023), must accurately represent these cycles under different  
61 environmental scenarios to reliably simulate carbon and nitrogen fluxes (Hungate *et al.*, 2003;  
62 Prentice *et al.*, 2015). While including coupled carbon and nitrogen cycles was intended to  
63 improve terrestrial biosphere model reliability, the role of nitrogen availability and nitrogen  
64 acquisition strategy on leaf and whole plant responses to increasing atmospheric CO<sub>2</sub>  
65 concentrations remains uncertain (Davies-Barnard *et al.*, 2020), contributing to divergent future  
66 carbon and nitrogen flux simulations across terrestrial biosphere models (Friedlingstein *et al.*,  
67 2014; Wieder *et al.*, 2015; Arora *et al.*, 2020; Meyerholt *et al.*, 2020).

68 Over the past few decades, numerous studies have revealed consistent leaf and whole-  
69 plant responses to elevated CO<sub>2</sub> (eCO<sub>2</sub>). At the leaf level, C<sub>3</sub> plants grown under eCO<sub>2</sub> exhibit  
70 increased net photosynthesis rates compared to plants grown under ambient CO<sub>2</sub> (aCO<sub>2</sub>)  
71 (Ainsworth & Long, 2005; Lee *et al.*, 2011; Poorter *et al.*, 2022). These patterns correspond with  
72 reduced mass- and area-based leaf nitrogen content, increased leaf mass per area, reduced  
73 stomatal conductance, and reduced photosynthetic capacity, yielding increased photosynthetic  
74 nitrogen-use efficiency and water-use efficiency (Curtis, 1996; Drake *et al.*, 1997; Ainsworth &  
75 Long, 2005; Ainsworth & Rogers, 2007; Lee *et al.*, 2011; Pastore *et al.*, 2019; Poorter *et al.*,  
76 2022). At the whole-plant level, C<sub>3</sub> plants grown under eCO<sub>2</sub> exhibit increased total leaf area,  
77 which supports greater net primary productivity and total biomass compared to plants grown  
78 under aCO<sub>2</sub> (Ainsworth *et al.*, 2002; Ainsworth & Rogers, 2007; Poorter *et al.*, 2022).

79 Despite consistent plant responses to eCO<sub>2</sub> documented across experiments, mechanisms  
80 that drive these responses remain unresolved. Some have hypothesized that plant responses to  
81 eCO<sub>2</sub> are constrained by nitrogen availability, as nitrogen availability limits net primary  
82 productivity globally (LeBauer & Treseder, 2008). The progressive nitrogen limitation  
83 hypothesis predicts that eCO<sub>2</sub> increases plant nitrogen uptake to support greater net primary  
84 productivity, which causes nitrogen availability to decline over time (Luo *et al.*, 2004). The

85 hypothesis predicts that this response should enhance positive effects of eCO<sub>2</sub> on net primary  
86 productivity and growth under eCO<sub>2</sub> over short time scales that dampen with time as nitrogen  
87 becomes more limiting and stored in longer-lived tissues. Growth responses to eCO<sub>2</sub> expected  
88 from the progressive nitrogen limitation hypothesis have received some support from free-air  
89 CO<sub>2</sub> enrichment experiments (Reich *et al.*, 2006; Norby *et al.*, 2010), though these patterns are  
90 not consistently observed (Finzi *et al.*, 2006; Moore *et al.*, 2006; Liang *et al.*, 2016).

91 Assuming positive relationships between soil nitrogen availability, leaf nitrogen content,  
92 and photosynthetic capacity (Field & Mooney, 1986; Evans, 1989), the progressive nitrogen  
93 limitation hypothesis implies that reductions in nitrogen availability over time might explain why  
94 C<sub>3</sub> plants grown under eCO<sub>2</sub> exhibit decreased leaf nitrogen content and photosynthetic capacity.  
95 However, free-air CO<sub>2</sub> enrichment experiments show that reductions in leaf nitrogen content and  
96 photosynthetic capacity due to eCO<sub>2</sub> are decoupled from changes in nitrogen availability (Crous  
97 *et al.*, 2010; Lee *et al.*, 2011; Pastore *et al.*, 2019). Additionally, aboveground conditions that  
98 alter the demand for building and maintaining photosynthetic enzymes may be a stronger  
99 determinant of variance in leaf nitrogen and photosynthetic capacity across environmental  
100 gradients (Dong *et al.*, 2017, 2020, 2022a; Paillassa *et al.*, 2020; Peng *et al.*, 2021; Waring *et al.*,  
101 2023). Thus, leaf photosynthetic responses to eCO<sub>2</sub> may be a product of altered demand to build  
102 and maintain photosynthetic enzymes and not due to changes in nitrogen availability.

103 Eco-evolutionary optimality theory provides a framework for understanding how demand  
104 for building and maintaining photosynthetic enzymes dictates leaf photosynthetic responses to  
105 eCO<sub>2</sub> (Harrison *et al.*, 2021). Merging photosynthetic least-cost (Wright *et al.*, 2003; Prentice *et*  
106 *al.*, 2014) and optimal coordination (Chen *et al.*, 1993; Maire *et al.*, 2012) theories, eco-  
107 evolutionary optimality theory posits that reduced leaf nitrogen allocation due to eCO<sub>2</sub> is the  
108 downstream result of a stronger downregulation in the maximum rate of Ribulose-1,5-  
109 bisphosphate (RuBP) carboxylase/oxygenase (Rubisco) carboxylation ( $V_{cmax}$ ) than the maximum  
110 rate of electron transport for RuBP regeneration ( $J_{max}$ ), which reduces leaf nitrogen demand for  
111 building and maintaining photosynthetic enzymes. The theory predicts that plants should  
112 optimize leaf nitrogen allocation to photosynthetic capacity to make more efficient use of  
113 available light while avoiding overinvestment in Rubisco, which has high nitrogen costs to build  
114 and maintain (Evans, 1989; Evans & Clarke, 2019). Such responses to eCO<sub>2</sub> increase  
115 photosynthetic nitrogen-use efficiency and increase net photosynthesis rates through increasingly

116 equal co-limitation of Rubisco carboxylation and electron transport for RuBP regeneration (Chen  
117 *et al.*, 1993; Maire *et al.*, 2012; Wang *et al.*, 2017; Smith *et al.*, 2019). The expected optimal leaf  
118 response to eCO<sub>2</sub> has received some empirical support (Crous *et al.*, 2010; Lee *et al.*, 2011;  
119 Smith & Keenan, 2020; Dong *et al.*, 2022b), though no studies have connected these patterns  
120 with concurrently measured whole-plant responses.

121 The eco-evolutionary optimality hypothesis deviates from the progressive nitrogen  
122 limitation hypothesis by indicating that changes in leaf nitrogen demand to build and maintain  
123 photosynthetic enzymes drive leaf-level responses to eCO<sub>2</sub> independent of changes in soil  
124 nitrogen availability. However, the eco-evolutionary optimality hypothesis does not discount the  
125 role of soil nitrogen availability on whole-plant responses to eCO<sub>2</sub>, where the expected optimal  
126 strategy in response to eCO<sub>2</sub> is to allocate surplus nitrogen not needed to satisfy demand to build  
127 and maintain photosynthetic enzymes toward the construction of a greater quantity of optimally  
128 coordinated leaves and other plant organs. Thus, whether patterns expected from the progressive  
129 nitrogen limitation hypothesis or eco-evolutionary optimality theory control plant responses to  
130 eCO<sub>2</sub> may be a matter of scale, where leaf nitrogen demand to build and maintain photosynthetic  
131 enzymes determines leaf-level responses to eCO<sub>2</sub> and nitrogen availability regulates whole-plant  
132 responses to eCO<sub>2</sub>.

133 Plants allocate carbon belowground in exchange for nutrients through different nutrient  
134 acquisition strategies, including direct uptake pathways or symbioses with mycorrhizal fungi and  
135 symbiotic nitrogen-fixing bacteria. Carbon costs to acquire nitrogen, or the amount of carbon  
136 plants allocate belowground per unit of nitrogen acquired, vary in species with different nitrogen  
137 acquisition strategies and are dependent on environmental factors such as atmospheric CO<sub>2</sub>,  
138 temperature, light availability, and nutrient availability (Brzostek *et al.*, 2014; Terrer *et al.*, 2018;  
139 Perkowski *et al.*, 2021). Therefore, it is important to consider nitrogen acquisition strategy when  
140 examining the effects of nitrogen availability on plant responses to eCO<sub>2</sub>. Few studies account  
141 for acquisition strategy when considering the role of nitrogen availability on leaf and whole-plant  
142 responses to eCO<sub>2</sub> (Terrer *et al.*, 2018; Smith & Keenan, 2020). Such studies found that nitrogen  
143 acquisition strategies with reduced carbon costs to acquire nitrogen may buffer the effect of  
144 nitrogen limitation at the whole-plant level (Terrer *et al.*, 2018), but leaf-level responses remain  
145 inconsistent (Terrer *et al.*, 2018; Smith & Keenan, 2020).

146 Here, *Glycine max* L. (Merr.) seedlings were grown under full-factorial combinations of  
147 two CO<sub>2</sub> concentrations, two inoculation treatments, and nine soil nitrogen fertilization  
148 treatments to reconcile the role of nitrogen availability and demand on plant responses to eCO<sub>2</sub>.  
149 We used this experimental setup to test the following hypotheses:

- 150 (1) Following eco-evolutionary optimality theory, eCO<sub>2</sub> will downregulate  $V_{cmax}$  more  
151 strongly than  $J_{max}$ , increasing the ratio of  $J_{max}$  to  $V_{cmax}$  and allowing increased net  
152 photosynthesis rates to approach equal co-limitation of Rubisco carboxylation and  
153 electron transport for RuBP regeneration. Leaf photosynthetic responses to eCO<sub>2</sub> will be  
154 independent of nitrogen fertilization and inoculation treatment.
- 155 (2) Following the progressive nitrogen limitation hypothesis, nitrogen fertilization will  
156 enhance the positive effect of eCO<sub>2</sub> on total leaf area and total biomass due to increased  
157 plant nitrogen uptake and reduced carbon costs to acquire nitrogen. Inoculation with  
158 symbiotic nitrogen-fixing bacteria will enhance positive growth responses to eCO<sub>2</sub>.  
159 However, these responses will only be apparent under low nitrogen fertilization, where  
160 individuals will invest more strongly in symbiotic nitrogen fixation.

161

## 162 Methods

### 163 Seed treatments and experimental design

164 *Glycine max* seeds were planted in 144 6-liter surface sterilized pots (NS-600, Nursery Supplies,  
165 Orange, CA, USA) containing a steam-sterilized 70:30 volume: volume mix of *Sphagnum* peat  
166 moss (Premier Horticulture, Quakertown, PA, USA) to sand (Pavestone, Atlanta, GA, USA).  
167 Before planting, all *G. max* seeds were surface sterilized in 2% sodium hypochlorite for 3  
168 minutes, followed by three 3-minute washes with ultrapure water (MilliQ 7000; MilliporeSigma,  
169 Burlington, MA USA). Subsets of surface-sterilized seeds were inoculated with *Bradyrhizobium*  
170 *japonicum* (Verdesian N-Dure™ Soybean, Cary, NC, USA) in a slurry following manufacturer  
171 recommendations (3.12 g inoculant and 241 g ultrapure water per 1 kg seed).

172 Seventy-two pots were randomly planted with surface-sterilized seeds inoculated with *B.*  
173 *japonicum*, while the remaining 72 pots were planted with surface-sterilized uninoculated seeds.  
174 Thirty-six pots in each inoculation treatment were placed in one of two atmospheric CO<sub>2</sub>  
175 treatments (420, 1000  $\mu\text{mol mol}^{-1}$  CO<sub>2</sub>). Plants in each unique inoculation-by-CO<sub>2</sub> treatment  
176 combination received one of nine nitrogen fertilization treatments equivalent to 0 (0 mM), 35

177 (2.5 mM), 70 (5 mM), 105 (7.5 mM), 140 (10 mM), 210 (15 mM), 280 (20 mM), 350 (25 mM),  
178 or 630 ppm (45 mM) N. Nitrogen fertilization treatments were created using a modified  
179 Hoagland's solution (Hoagland & Arnon, 1950) designed to keep concentrations of all other  
180 macronutrients and micronutrients equivalent across treatments (Table S1). Plants received the  
181 same nitrogen fertilization treatment twice per week in 150 mL doses as topical agents to the soil  
182 surface.

183

184 *Growth chamber conditions*

185 Plants were randomly placed in one of six Percival LED-41L2 growth chambers (Percival  
186 Scientific Inc., Perry, IA, USA) over two experimental iterations due to chamber space  
187 limitation. The first iteration included all plants grown under eCO<sub>2</sub>, while the second included all  
188 plants grown under aCO<sub>2</sub>. Average ( $\pm$  SD) CO<sub>2</sub> concentrations across chambers throughout the  
189 experiment were  $439 \pm 5 \text{ } \mu\text{mol mol}^{-1}$  CO<sub>2</sub> for the ambient treatment and  $989 \pm 4 \text{ } \mu\text{mol mol}^{-1}$  CO<sub>2</sub>  
190 for the elevated treatment.

191 Daytime growth conditions were simulated using a 16-hour photoperiod, with incoming  
192 light radiation set to chamber maximum (mean $\pm$ SD:  $1230 \pm 12 \text{ } \mu\text{mol m}^{-2} \text{ s}^{-1}$  across chambers), air  
193 temperature set to 25°C, and relative humidity set to 50%. The remaining 8-hour period  
194 simulated nighttime growing conditions, with incoming light radiation set to  $0 \text{ } \mu\text{mol m}^{-2} \text{ s}^{-1}$ ,  
195 chamber temperature set to 17°C, and relative humidity set to 50%. Transitions between daytime  
196 and nighttime growing conditions were simulated by ramping incoming light radiation in 45-  
197 minute increments and temperature in 90-minute increments over 3 hours (Table S2).

198 Plants grew under average ( $\pm$  SD) daytime light intensity of  $1049 \pm 27 \text{ } \mu\text{mol m}^{-2} \text{ s}^{-1}$ ,  
199 including ramping periods. In the eCO<sub>2</sub> iteration, plants grew under  $24.0 \pm 0.2^\circ\text{C}$  during the day,  
200  $16.4 \pm 0.8^\circ\text{C}$  during the night, and  $51.6 \pm 0.4\%$  relative humidity. In the aCO<sub>2</sub> iteration, plants grew  
201 under  $23.9 \pm 0.2^\circ\text{C}$  during the day,  $16.0 \pm 1.4^\circ\text{C}$  during the night, and  $50.3 \pm 0.2\%$  relative humidity.  
202 Any differences in climate conditions across the six chambers were accounted for by shuffling  
203 the same group of plants throughout the growth chambers. This process was done by iteratively  
204 moving the group of plants on the top rack of a chamber to the bottom rack of the same chamber  
205 while simultaneously moving the group of plants on the bottom rack of a chamber to the top rack  
206 of the adjacent chamber. Plants were moved within and across chambers daily during each  
207 experiment iteration.

208

209 *Leaf gas exchange measurements*

210 Leaf gas exchange measurements were collected on the seventh week of development, before the  
211 onset of reproduction. All gas exchange measurements were collected on the center leaf of the  
212 most recent fully expanded trifoliate leaf set using LI-6800 portable photosynthesis machines  
213 configured with a 6800-01A fluorometer head and 6 cm<sup>2</sup> aperture (LI-COR Biosciences,  
214 Lincoln, NE, USA). Specifically, net photosynthesis rates ( $A_{\text{net}}$ ;  $\mu\text{mol m}^{-2} \text{s}^{-1}$ ), stomatal  
215 conductance rates ( $g_{\text{sw}}$ ;  $\text{mol m}^{-2} \text{s}^{-1}$ ), and intercellular CO<sub>2</sub> concentrations ( $C_i$ ;  $\mu\text{mol mol}^{-1}$ ) were  
216 measured across a range of atmospheric CO<sub>2</sub> concentrations (i.e., an  $A_{\text{net}}/C_i$  curve) using the  
217 Dynamic Assimilation™ Technique. The Dynamic Assimilation™ Technique corresponds well  
218 with traditional steady-state  $A_{\text{net}}/C_i$  curves in *G. max* (Saathoff & Welles, 2021).  $A_{\text{net}}/C_i$  curves  
219 were generated along a reference CO<sub>2</sub> ramp down from 420  $\mu\text{mol mol}^{-1}$  CO<sub>2</sub> to 20  $\mu\text{mol mol}^{-1}$   
220 CO<sub>2</sub>, followed by a ramp up from 420  $\mu\text{mol mol}^{-1}$  CO<sub>2</sub> to 1620  $\mu\text{mol mol}^{-1}$  CO<sub>2</sub> after a 90-  
221 second wait period at 420  $\mu\text{mol mol}^{-1}$  CO<sub>2</sub>. The ramp rate for each curve was set to 200  $\mu\text{mol}$   
222  $\text{mol}^{-1} \text{min}^{-1}$ , logging every five seconds, generating 96 data points per response curve. All  $A_{\text{net}}/C_i$   
223 curves were conducted after  $A_{\text{net}}$  and  $g_{\text{sw}}$  stabilized in a LI-6800 cuvette set to a 500  $\text{mol s}^{-1}$  flow  
224 rate, 10000 rpm mixing fan speed, 1.5 kPa vapor pressure deficit, 25°C leaf temperature, 2000  
225  $\mu\text{mol m}^{-2} \text{s}^{-1}$  incoming light radiation, and initial reference CO<sub>2</sub> set to 420  $\mu\text{mol mol}^{-1}$ .

226 Snapshot  $A_{\text{net}}$  measurements were extracted from each  $A_{\text{net}}/C_i$  curve, both at a common  
227 CO<sub>2</sub> concentration, 420  $\mu\text{mol mol}^{-1}$  CO<sub>2</sub> ( $A_{\text{net},420}$ ;  $\mu\text{mol m}^{-2} \text{s}^{-1}$ ), and growth CO<sub>2</sub> concentration,  
228 420 and 1000  $\mu\text{mol mol}^{-1}$  CO<sub>2</sub> ( $A_{\text{net,growth}}$ ;  $\mu\text{mol m}^{-2} \text{s}^{-1}$ ). Dark respiration ( $R_d$ ;  $\mu\text{mol m}^{-2} \text{s}^{-1}$ )  
229 measurements were collected on the same leaf used to generate  $A_{\text{net}}/C_i$  curves following at least  
230 30 minutes of darkness. Measurements were collected on a 5-second log interval for 60 seconds  
231 after the leaf stabilized in a LI-6800 cuvette set to a 500  $\text{mol s}^{-1}$  flow rate, 10000 rpm mixing fan  
232 speed, 1.5 kPa vapor pressure deficit, 25°C leaf temperature, and 420  $\mu\text{mol mol}^{-1}$  reference CO<sub>2</sub>  
233 concentration (regardless of CO<sub>2</sub> treatment), with incoming light radiation set to 0  $\mu\text{mol m}^{-2} \text{s}^{-1}$ .  
234 A single dark respiration value was determined for each leaf by calculating the mean dark  
235 respiration value across the logging interval.

236

237 *A/C<sub>i</sub> curve-fitting and parameter estimation*

238  $A_{\text{net}}/C_i$  curves were fit using the 'fitaci' function in the 'plantecophys' R package(Duursma,  
 239 2015). This function estimates the maximum rate of Rubisco carboxylation ( $V_{\text{cmax}}$ ;  $\mu\text{mol m}^{-2} \text{s}^{-1}$ )  
 240 and maximum rate of electron transport for RuBP regeneration ( $J_{\text{max}}$ ;  $\mu\text{mol m}^{-2} \text{s}^{-1}$ ) based on the  
 241 Farquhar et al. (1980) biochemical model of C<sub>3</sub> photosynthesis. Triose phosphate utilization  
 242 (TPU) limitation was included as an additional rate-limiting step after visually observing clear  
 243 TPU limitation for most curves. All curve fits included measured dark respiration values. As  
 244  $A_{\text{net}}/C_i$  curves were generated using a common leaf temperature (25°C), curves were fit using  
 245 Michaelis-Menten coefficients for Rubisco affinity to CO<sub>2</sub> ( $K_c$ ;  $\mu\text{mol mol}^{-1}$ ) and O<sub>2</sub> ( $K_o$ ;  $\text{mmol}$   
 246  $\text{mol}^{-1}$ ), and the CO<sub>2</sub> compensation point ( $T^*$ ;  $\mu\text{mol mol}^{-1}$ ) reported in Bernacchi et al. (2001).  
 247 Specifically,  $K_c$  was set to 404.9  $\mu\text{mol mol}^{-1}$ ,  $K_o$  was set to 278.4  $\mu\text{mol mol}^{-1}$ , and  $T^*$  was set to  
 248 42.75  $\mu\text{mol mol}^{-1}$ .  $V_{\text{cmax}}$ ,  $J_{\text{max}}$ , and  $R_d$  estimates are referenced throughout the rest of the paper as  
 249  $V_{\text{cmax}25}$ ,  $J_{\text{max}25}$ , and  $R_{d25}$ .

250

### 251 Leaf trait measurements

252 The leaf used for  $A_{\text{net}}/C_i$  curves and dark respiration measurements was harvested immediately  
 253 following gas exchange measurements. Images of each focal leaf were curated using a flat-bed  
 254 scanner to determine fresh leaf area using the 'LeafArea' R package (Katabuchi, 2015), which  
 255 automates leaf area calculations using ImageJ software (Schneider *et al.*, 2012). Post-processed  
 256 images were visually assessed to check against errors in the automation process. Each leaf was  
 257 dried at 65°C for at least 48 hours, weighed, and ground until homogenized. Leaf mass per area  
 258 ( $M_{\text{area}}$ ;  $\text{g m}^{-2}$ ) was calculated as the ratio of dry leaf biomass to fresh leaf area. Leaf nitrogen  
 259 content ( $N_{\text{mass}}$ ;  $\text{gN g}^{-1}$ ) was quantified using a subsample of ground and homogenized leaf tissue  
 260 through elemental combustion (Costech-4010, Costech, Inc., Valencia, CA, USA). Leaf nitrogen  
 261 content per unit leaf area ( $N_{\text{area}}$ ;  $\text{gN m}^{-2}$ ) was calculated by multiplying  $N_{\text{mass}}$  and  $M_{\text{area}}$ .  
 262 Photosynthetic nitrogen-use efficiency ( $PNUE_{\text{growth}}$ ;  $\mu\text{mol CO}_2 \text{ g}^{-1} \text{ N s}^{-1}$ ) was estimated as the  
 263 ratio of  $A_{\text{net,growth}}$  to  $N_{\text{area}}$ . Chlorophyll content was extracted from a second leaf in the same  
 264 trifoliolate leaf set as the leaf used to generate  $A_{\text{net}}/C_i$  curves and quantified using methods  
 265 described in Barnes *et al.* (1992) and Wellburn (1994). Detailed methods for chlorophyll  
 266 extractions are included in the *Supplemental Material*.

267 Subsamples of ground and homogenized leaf tissue were sent to the University of  
 268 California-Davis Stable Isotope Facility to determine leaf δ<sup>13</sup>C and δ<sup>15</sup>N using an elemental

269 analyzer (Elementar vario MICRO cube elemental analyzer; Elementar Analysensysteme GmbH,  
 270 Langenselbold, Germany) interfaced to an isotope ratio mass spectrometer (PDZ Europa 20-20  
 271 Isotope Ratio Mass Spectrometer, Sercon Ltd., Chestshire, UK). Leaf  $\delta^{13}\text{C}$  was used to estimate  
 272 the ratio of leaf intercellular CO<sub>2</sub> concentration to atmospheric CO<sub>2</sub> concentration ( $\chi$ , unitless),  
 273 summarized in the *Supplemental Material*. The percent of leaf nitrogen derived from the  
 274 atmosphere (%N<sub>dfa</sub>; %) was estimated following Andrews et al. (2011):

$$275 \quad \%N_{dfa} = \frac{\delta^{15}\text{N}_{direct} - \delta^{15}\text{N}_{sample}}{\delta^{15}\text{N}_{direct} - \delta^{15}\text{N}_{fixation}} \quad (1)$$

276 where  $\delta^{15}\text{N}_{direct}$  refers to  $\delta^{15}\text{N}$  from plants that acquired nitrogen only through direct uptake,  
 277  $\delta^{15}\text{N}_{sample}$  refers to an individual's leaf  $\delta^{15}\text{N}$ , and  $\delta^{15}\text{N}_{fixation}$  refers to  $\delta^{15}\text{N}$  from individuals  
 278 entirely reliant on nitrogen fixation.  $\delta^{15}\text{N}_{direct}$  was calculated as the mean leaf  $\delta^{15}\text{N}$  of  
 279 uninoculated individuals for each nitrogen fertilization-by-CO<sub>2</sub> treatment combination. Any  
 280 individual with visual evidence of root nodule formation or nodule initiation was omitted from  
 281  $\delta^{15}\text{N}_{direct}$ .  $\delta^{15}\text{N}_{fixation}$  was calculated for each CO<sub>2</sub> treatment using the mean leaf  $\delta^{15}\text{N}$  of  
 282 inoculated individuals that received 0 ppm N.  $\delta^{15}\text{N}_{fixation}$  was not calculated for each nitrogen  
 283 fertilization-by-CO<sub>2</sub> treatment combination due to decreased reliance on symbiotic nitrogen  
 284 fixation with increasing nitrogen fertilization (Rastetter *et al.*, 2001; Andrews *et al.*, 2011;  
 285 Perkowski *et al.*, 2021).

286

#### 287 *Whole-plant measurements*

288 All individuals were harvested, and biomass of major organ types (leaves, stems, roots, and  
 289 nodules when present) were separated immediately following gas exchange measurements. Fresh  
 290 leaf area of all harvested leaves was measured using a LI-3100C (LI-COR Biosciences, Lincoln,  
 291 Nebraska, USA). Total fresh leaf area (cm<sup>2</sup>) was calculated as the sum of all leaf areas, including  
 292 the leaf used for gas exchange and chlorophyll extractions. Harvested material was separately  
 293 dried in an oven set to 65°C for at least 48 hours to a constant mass, weighed, and ground to  
 294 homogeneity. Leaves and root nodules were ground using a mortar and pestle, while stems and  
 295 roots were ground using an E3300 Single Speed Mini Cutting Mill (Eberbach Corp., MI, USA).  
 296 Total biomass (g) was calculated as the sum of dry leaf, stem, root, and root nodule biomass.  
 297 Carbon and nitrogen content was measured for each organ type through elemental combustion  
 298 (Costech-4010, Costech, Inc., Valencia, CA, USA) using ground and homogenized organ tissue

299 subsamples. The ratio of root nodule biomass to root biomass was calculated as an additional  
300 indicator of investment toward nitrogen fixation.

301 Carbon costs to acquire nitrogen were quantified as the ratio of belowground carbon  
302 biomass to total nitrogen biomass ( $N_{\text{cost}}$ ; gC gN<sup>-1</sup>) (Perkowski *et al.*, 2021). Belowground carbon  
303 biomass ( $C_{\text{bg}}$ ; gC) was calculated as the sum of root and root nodule carbon biomass. Root  
304 carbon biomass and root nodule carbon biomass were calculated as the product of the organ  
305 biomass and respective organ carbon content. Total nitrogen biomass ( $N_{\text{wp}}$ ; gN) was calculated  
306 as the sum of total leaf, stem, root, and root nodule nitrogen biomass. Leaf, stem, root, and root  
307 nodule nitrogen biomass was calculated as the product of the organ biomass and respective organ  
308 nitrogen content. This calculation does not account for additional carbon costs associated with  
309 respiration, root exudation, or root turnover and may underestimate carbon costs to acquire  
310 nitrogen (Perkowski *et al.*, 2021).

311

### 312 *Statistical analyses*

313 Uninoculated plants with substantial root nodule formation (root nodule biomass: root biomass  
314 values greater than 0.05 g g<sup>-1</sup>) were removed from analyses assuming that plants were either  
315 incompletely sterilized or were colonized by neighboring plants in the chamber. This decision  
316 resulted in the removal of sixteen plants from the analysis: two plants in the eCO<sub>2</sub> treatment that  
317 received 35 ppm N, three plants in the eCO<sub>2</sub> treatment that received 70 ppm N, one plant in the  
318 eCO<sub>2</sub> treatment that received 210 ppm N, two plants in the eCO<sub>2</sub> treatment that received 280  
319 ppm N, two plants in the aCO<sub>2</sub> treatment that received 0 ppm N, three plants in the aCO<sub>2</sub>  
320 treatment that received 70 ppm N, two plants in the aCO<sub>2</sub> treatment that received 105 ppm N,  
321 and one plant in the aCO<sub>2</sub> treatment that received 280 ppm N.

322 A series of linear mixed-effects models were built to investigate the impacts of CO<sub>2</sub>  
323 concentration, nitrogen fertilization, and inoculation on *G. max* leaf nitrogen allocation, gas  
324 exchange, whole-plant growth, and investment in nitrogen fixation. All models included CO<sub>2</sub>  
325 treatment as a categorical fixed effect, inoculation treatment as a categorical fixed effect, and  
326 nitrogen fertilization as a continuous fixed effect, with all possible interaction terms between all  
327 three fixed effects also included. Models accounted for climatic differences between chambers  
328 across experiment iterations by including a random intercept term that nested the starting  
329 chamber rack by CO<sub>2</sub> treatment. Models with this independent variable structure were created for

330 each of the following dependent variables:  $N_{\text{area}}$ ,  $M_{\text{area}}$ ,  $N_{\text{mass}}$ ,  $\text{Chl}_{\text{area}}$ ,  $A_{\text{net},420}$ ,  $A_{\text{net,growth}}$ ,  $V_{\text{cmax}25}$ ,  
 331  $J_{\text{max}25}$ ,  $J_{\text{max}25}:V_{\text{cmax}25}$ ,  $R_{\text{d}25}$ ,  $\text{PNUE}_{\text{growth}}$ ,  $\chi$ , total leaf area, total biomass,  $N_{\text{cost}}$ ,  $C_{\text{bg}}$ ,  $N_{\text{wp}}$ ,  $\%N_{\text{dfa}}$ ,  
 332 root nodule biomass: root biomass, root nodule biomass, and root biomass.

333 Shapiro-Wilk tests of normality were used to assess whether linear mixed-effects models  
 334 satisfied residual normality assumptions. Models for  $N_{\text{area}}$ ,  $N_{\text{mass}}$ ,  $\text{Chl}_{\text{area}}$ ,  $A_{\text{net},420}$ ,  $A_{\text{net,growth}}$ ,  
 335  $V_{\text{cmax}25}$ ,  $J_{\text{max}25}$ ,  $J_{\text{max}25}:V_{\text{cmax}25}$ ,  $R_{\text{d}25}$ ,  $\text{PNUE}_{\text{growth}}$ ,  $\chi$ , total leaf area, and  $N_{\text{cost}}$  each satisfied residual  
 336 normality assumptions without data transformation. Models for  $M_{\text{area}}$ , total biomass, and  $C_{\text{bg}}$   
 337 satisfied residual normality assumptions with a natural log data transformation. Models for  $N_{\text{wp}}$ ,  
 338 root nodule biomass: root biomass, root nodule biomass, root biomass, and  $\%N_{\text{dfa}}$  satisfied  
 339 residual normality assumptions with a square root data transformation.

340 In all models, the ‘lmer’ function in the ‘lme4’ R package (Bates *et al.*, 2015) was used to  
 341 fit each model, and the ‘Anova’ function in the ‘car’ R package (Fox & Weisberg, 2019) was  
 342 used to calculate Type II Wald's  $\chi^2$  and determine the significance ( $\alpha=0.05$ ) of each fixed effect  
 343 coefficient. The ‘emmeans’ R package (Lenth, 2019) was used to conduct post-hoc comparisons  
 344 using Tukey's tests, where degrees of freedom were approximated using the Kenward-Roger  
 345 approach (Kenward & Roger, 1997). Trendlines and error ribbons representing the 95%  
 346 confidence intervals were drawn in all figures using ‘emmeans’ outputs across the range in  
 347 nitrogen fertilization values. All analyses and plots were conducted in R version 4.1.0 (R Core  
 348 Team, 2021). Model results for  $\text{PNUE}_{\text{growth}}$ ,  $\chi$ ,  $C_{\text{bg}}$ ,  $N_{\text{wp}}$ , root nodule biomass: root biomass, root  
 349 nodule biomass, and root biomass are reported in the *Supplemental Material* (Tables S3-S6;  
 350 Figs. S3-S6).

351

## 352 Results

### 353 Leaf nitrogen content

354 eCO<sub>2</sub> reduced  $N_{\text{area}}$ ,  $N_{\text{mass}}$ , and  $\text{Chl}_{\text{area}}$  by 29%, 50%, and 31%, respectively, and increased  $M_{\text{area}}$   
 355 by 44% ( $p<0.001$  in all cases; Table 1). Interactions between nitrogen fertilization and CO<sub>2</sub>  
 356 ( $p<0.05$  in all cases; Table 1) indicated that the positive effects of increasing nitrogen  
 357 fertilization on  $N_{\text{area}}$ ,  $N_{\text{mass}}$ , and  $M_{\text{area}}$  ( $p<0.001$  in all cases; Table 1) were stronger under aCO<sub>2</sub>  
 358 than eCO<sub>2</sub> (Tukey test of the nitrogen fertilization-trait slope between CO<sub>2</sub>:  $p<0.05$  in all cases).  
 359 These responses resulted in a stronger reduction in  $N_{\text{area}}$  and  $N_{\text{mass}}$  and a stronger increase in  $M_{\text{area}}$   
 360 under eCO<sub>2</sub> with increasing nitrogen fertilization than aCO<sub>2</sub> (Fig. S1). Nitrogen fertilization did

361 not modify reductions in  $Chl_{area}$  due to eCO<sub>2</sub> (Tukey test of the nitrogen fertilization- $Chl_{area}$  slope  
362 between CO<sub>2</sub> treatments:  $p>0.05$ ).

363 An interaction between inoculation and CO<sub>2</sub> ( $p<0.05$ ; Table 1) indicated that reductions  
364 in  $N_{area}$  due to eCO<sub>2</sub> were stronger in uninoculated plants (36% reduction; Tukey test of the CO<sub>2</sub>  
365 effect in uninoculated plants:  $p<0.001$ ) than inoculated plants (22% reduction; Tukey test of the  
366 CO<sub>2</sub> effect in inoculated plants:  $p<0.001$ ). Inoculation did not modify  $N_{mass}$ ,  $M_{area}$ , or  $Chl_{area}$   
367 responses to eCO<sub>2</sub> (CO<sub>2</sub>-by-inoculation interaction:  $p>0.05$  in all cases; Table 1). However, an  
368 interaction between nitrogen fertilization and inoculation ( $p<0.05$  in all cases; Table 1; Figs. 1a-  
369 d) indicated that positive effects of increasing nitrogen fertilization on  $N_{area}$ ,  $N_{mass}$ ,  $M_{area}$ , and  
370  $Chl_{area}$  ( $p<0.001$  in all cases; Table 1) were stronger in uninoculated plants compared to  
371 inoculated plants (Tukey test of the nitrogen fertilization-trait slope between inoculation  
372 treatments:  $p<0.05$  in all cases).

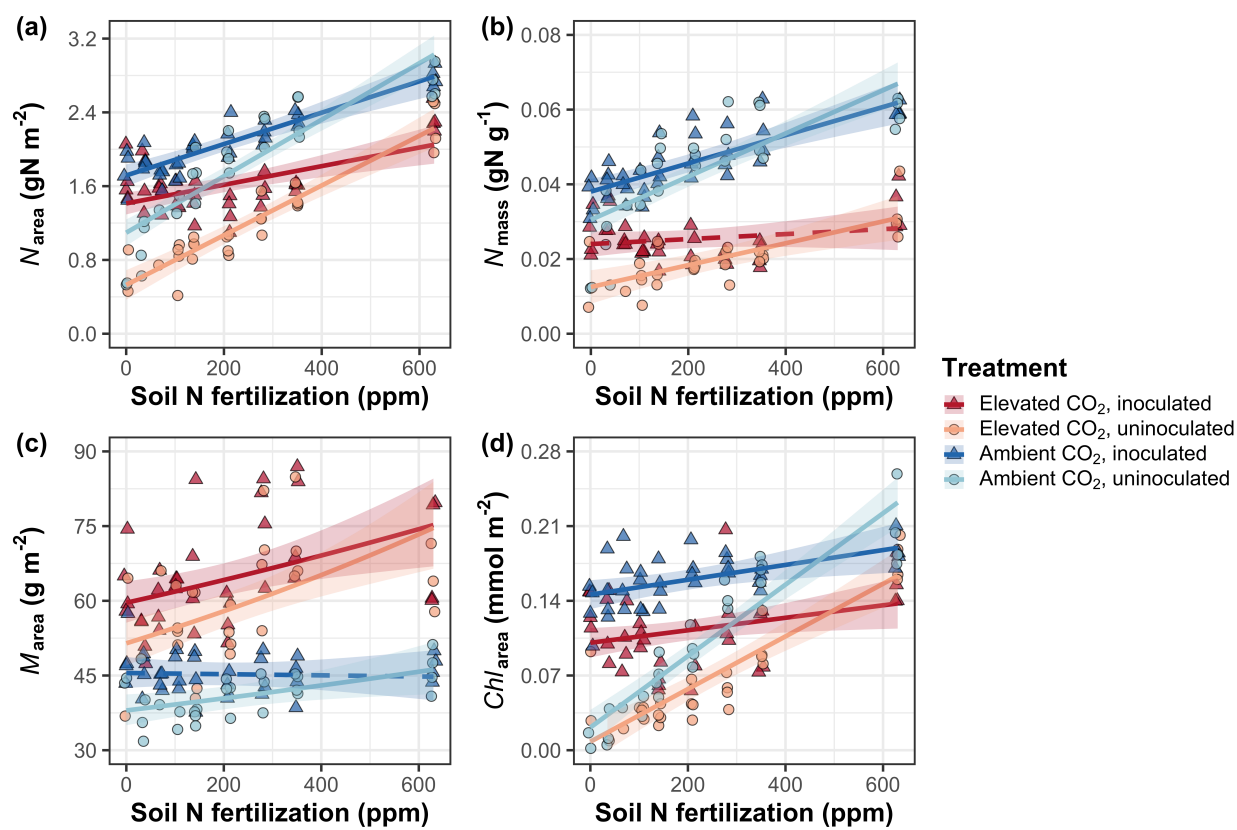
373

374 **Table 1** Effects of CO<sub>2</sub> concentration, inoculation, and nitrogen fertilization on leaf nitrogen allocation\*

		<i>N<sub>area</sub></i>		<i>N<sub>mass</sub></i>		<i>M<sub>area</sub><sup>a</sup></i>		<i>Chl<sub>area</sub></i>	
	df	$\chi^2$	<i>p</i>	$\chi^2$	<i>p</i>	$\chi^2$	<i>p</i>	$\chi^2$	<i>p</i>
CO <sub>2</sub>	1	155.908	<b>&lt;0.001</b>	272.362	<b>&lt;0.001</b>	151.319	<b>&lt;0.001</b>	69.233	<b>&lt;0.001</b>
Inoculation (I)	1	86.029	<b>&lt;0.001</b>	15.576	<b>&lt;0.001</b>	19.158	<b>&lt;0.001</b>	136.341	<b>&lt;0.001</b>
N fertilization (N)	1	316.408	<b>&lt;0.001</b>	106.659	<b>&lt;0.001</b>	21.440	<b>&lt;0.001</b>	163.111	<b>&lt;0.001</b>
CO <sub>2</sub> *I	1	4.729	<b>0.030</b>	2.025	0.155	0.029	0.866	2.102	0.147
CO <sub>2</sub> *N	1	5.723	<b>0.017</b>	22.542	<b>&lt;0.001</b>	7.619	<b>0.006</b>	2.999	0.083
I*N	1	43.381	<b>&lt;0.001</b>	11.137	<b>0.001</b>	5.022	<b>0.025</b>	75.769	<b>&lt;0.001</b>
CO <sub>2</sub> *I*N	1	0.489	0.484	0.041	0.839	0.208	0.649	2.144	0.143

375 \*Significance determined using Type II Wald  $\chi^2$  tests ( $\alpha=0.05$ ). *P*-values less than 0.05 are in bold. A superscript “a” is included after  
 376 trait labels to indicate if models were fit with natural log-transformed response variables. Key: df=degrees of freedom,  $\chi^2$ =Wald chi-  
 377 square test statistic, *N<sub>area</sub>*=leaf nitrogen content per unit leaf area (g N m<sup>-2</sup>), *N<sub>mass</sub>*=leaf nitrogen content (g N g<sup>-1</sup>), *M<sub>area</sub>*=leaf mass per  
 378 unit leaf area (g m<sup>-2</sup>).

379

380 **Figure 1**

381  
382 **Figure 1** Effects of CO<sub>2</sub> concentration, nitrogen fertilization, and inoculation on leaf nitrogen per  
383 unit leaf area (a), leaf nitrogen per unit leaf mass (b), leaf mass per unit leaf area (c), and  
384 chlorophyll content per unit leaf area (d). Nitrogen fertilization is represented on the x-axis in all  
385 panels. Red shaded points and trendlines indicate plants grown under eCO<sub>2</sub>, while blue shaded  
386 points and trendlines indicate plants grown under aCO<sub>2</sub>. Light blue and red circular points and  
387 trendlines indicate measurements collected from uninoculated plants, while dark blue and red  
388 triangular points indicate measurements collected from inoculated plants. Solid trendlines  
389 indicate regression slopes that are different from zero ( $p < 0.05$ ), while dashed trendlines indicate  
390 slopes that are not distinguishable from zero ( $p > 0.05$ ).  
391

392 *Gas exchange*

393 eCO<sub>2</sub> decreased  $A_{net,420}$  by 17% ( $p<0.001$ ; Table 2) and increased  $A_{net,growth}$  by 33% ( $p<0.001$ ;  
 394 Table 2). Nitrogen fertilization did not modify effects of eCO<sub>2</sub> on  $A_{net,420}$  or  $A_{net,growth}$  (CO<sub>2</sub>-by-  
 395 nitrogen fertilization interaction:  $p>0.05$  in both cases; Table 2; Fig. 2a-b). Inoculation did not  
 396 modify  $A_{net,420}$  responses to eCO<sub>2</sub> (CO<sub>2</sub>-by-inoculation interaction:  $p>0.05$ ). However, an  
 397 interaction between CO<sub>2</sub> and inoculation ( $p<0.05$ ; Table 2) indicated that inoculated plants  
 398 experienced a stronger increase in  $A_{net,growth}$  due to eCO<sub>2</sub> (38% increase; Tukey test of the CO<sub>2</sub>  
 399 effect in inoculated plants:  $p<0.001$ ) compared to uninoculated plants (26% increase; Tukey test  
 400 of the CO<sub>2</sub> effect in uninoculated plants:  $p<0.05$ ). An interaction between nitrogen fertilization  
 401 and inoculation ( $p<0.001$  in both cases; Table 2) indicated that positive effects of increasing  
 402 nitrogen fertilization on  $A_{net,420}$  and  $A_{net,growth}$  ( $p<0.001$  in both cases; Table 2; Fig. 2a-b) were  
 403 stronger in uninoculated plants than inoculated plants (Tukey test comparing the nitrogen  
 404 fertilization-trait slope between inoculation treatments:  $p<0.001$  in both cases).

405 eCO<sub>2</sub> decreased  $V_{cmax25}$  and  $J_{max25}$  by 16% and 10%, respectively, increasing  
 406  $J_{max25}:V_{cmax25}$  by 8% ( $p<0.05$  in all cases; Table 2; Fig. 2c-e).  $V_{cmax25}$ ,  $J_{max25}$ , and  $J_{max25}:V_{cmax25}$   
 407 responses to eCO<sub>2</sub> were not modified by nitrogen fertilization (CO<sub>2</sub>-by-nitrogen fertilization  
 408 interaction:  $p>0.05$  in all cases; Table 2; Fig. 2c-e) or inoculation (CO<sub>2</sub>-by-inoculation  
 409 interaction:  $p>0.05$  in all cases; Table 2). An interaction between nitrogen fertilization and  
 410 inoculation ( $p<0.05$  in both cases; Table 2) indicated that positive effects of increasing nitrogen  
 411 fertilization on  $V_{cmax25}$  and  $J_{max25}$  ( $p<0.001$  in both cases; Table 2) and negative effects of  
 412 increasing nitrogen fertilization on  $J_{max25}:V_{cmax25}$  ( $p<0.001$ ; Table 2) were driven by uninoculated  
 413 plants (Tukey test of the nitrogen fertilization-trait slope in uninoculated plants:  $p<0.001$  in all  
 414 cases), as there was no effect of nitrogen fertilization on  $V_{cmax25}$ ,  $J_{max25}$ , or  $J_{max25}:V_{cmax25}$  in  
 415 inoculated plants (Tukey test of the nitrogen fertilization-trait slope in inoculated plants:  $p>0.05$   
 416 in all cases).

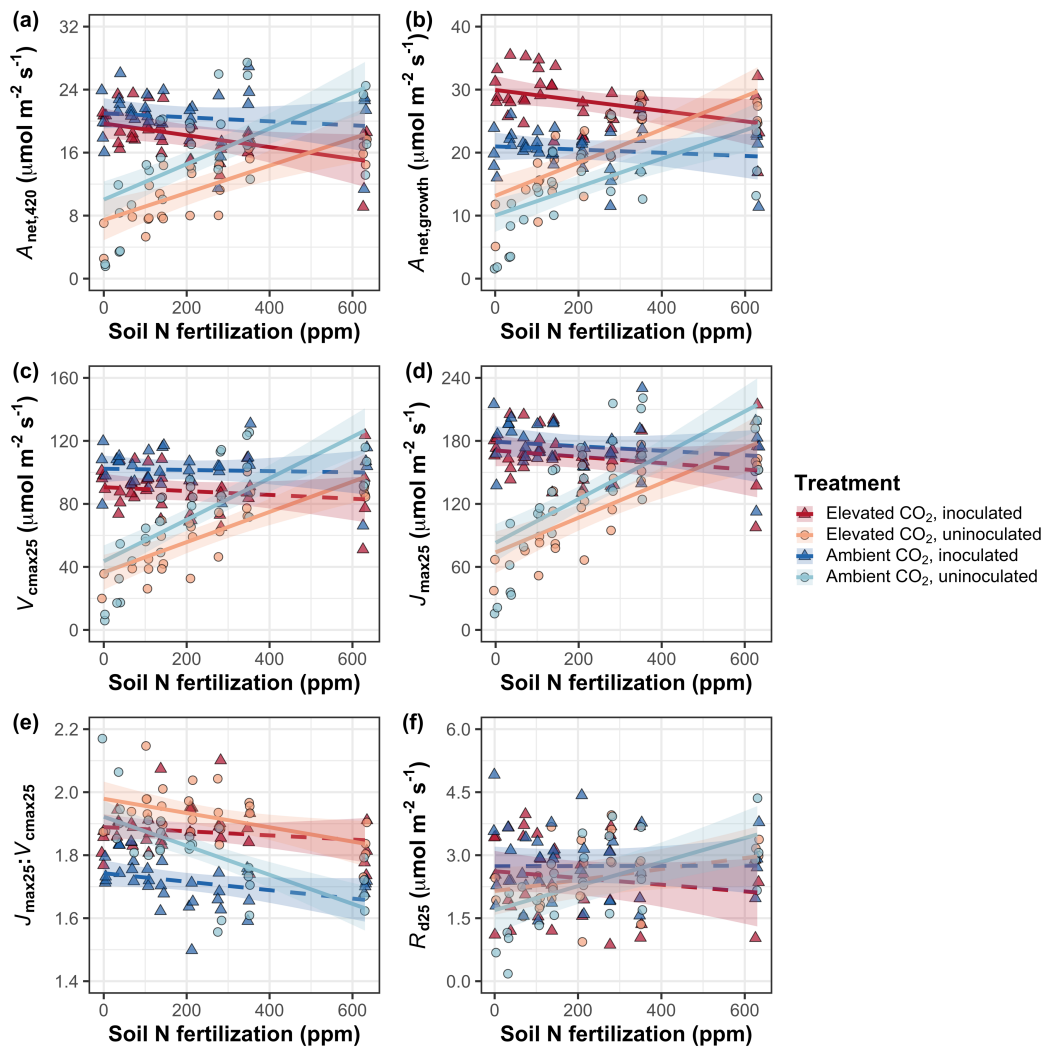
417 There was no effect of CO<sub>2</sub> concentration on  $R_{d25}$  ( $p>0.05$ ; Table 2). An interaction  
 418 between nitrogen fertilization and inoculation ( $p<0.001$ ; Table 2) indicated that the positive  
 419 effect of increasing nitrogen fertilization on  $R_{d25}$  ( $p<0.05$ ; Table 2) was driven by uninoculated  
 420 plants (Tukey test of the nitrogen fertilization- $R_{d25}$  slope in uninoculated plants:  $p<0.001$ ), as  
 421 there was no effect of nitrogen fertilization on  $R_{d25}$  in inoculated plants (Tukey test of the  
 422 nitrogen fertilization- $R_{d25}$  slope in inoculated plants:  $p>0.05$ ).

423 **Table 2** Effects of CO<sub>2</sub> concentration, inoculation, and nitrogen fertilization on leaf gas exchange\*

		<i>A</i> <sub>net,420</sub>		<i>A</i> <sub>net,growth</sub>		<i>V</i> <sub>cmax25</sub>		<i>J</i> <sub>max25</sub>	
	df	$\chi^2$	p	$\chi^2$	p	$\chi^2$	p	$\chi^2$	p
CO <sub>2</sub>	1	15.747	<0.001	52.716	<0.001	18.039	<0.001	6.042	0.014
Inoculation (I)	1	77.137	<0.001	83.008	<0.001	98.579	<0.001	85.064	<0.001
N fertilization (N)	1	11.986	<0.001	14.658	<0.001	37.053	<0.001	25.356	<0.001
CO <sub>2</sub> *I	1	1.032	0.310	5.634	0.018	0.065	0.799	0.667	0.414
CO <sub>2</sub> *N	1	1.998	0.158	0.135	0.713	1.758	0.185	0.742	0.389
I*N	1	46.800	<0.001	50.774	<0.001	60.394	<0.001	57.41	<0.001
CO <sub>2</sub> *I*N	1	0.002	0.964	1.332	0.248	0.748	0.387	0.377	0.539

	<i>J</i> <sub>max25:<i>V</i><sub>cmax25</sub></sub>		<i>R</i> <sub>d25</sub>		
	$\chi^2$	p	$\chi^2$	p	
CO <sub>2</sub>	1	92.010	<0.001	0.256	0.613
Inoculation (I)	1	27.768	<0.001	3.094	0.079
N fertilization (N)	1	28.147	<0.001	5.965	0.015
CO <sub>2</sub> *I	1	2.916	0.088	2.563	0.109
CO <sub>2</sub> *N	1	3.210	0.073	2.675	0.102
I*N	1	9.607	0.002	12.083	0.001
CO <sub>2</sub> *I*N	1	1.102	0.294	0.244	0.622

424 \*Significance determined using Type II Wald  $\chi^2$  tests ( $\alpha=0.05$ ). P-values less than 0.05 are in bold. Key: df=degrees of freedom,425  $\chi^2$ =Wald chi-square test statistic,  $A_{net}$ =net photosynthesis rate ( $\mu\text{mol m}^{-2} \text{s}^{-1}$ ),  $V_{cmax25}$ =maximum rate of Rubisco carboxylation at 25°C426 ( $\mu\text{mol m}^{-2} \text{s}^{-1}$ ),  $J_{max25}$ =maximum rate of electron transport for RuBP regeneration at 25°C ( $\mu\text{mol m}^{-2} \text{s}^{-1}$ ),  $J_{max25}:V_{cmax25}$ =ratio of  $J_{max25}$ 427 to  $V_{cmax25}$  (unitless),  $R_{d25}$ =dark respiration at 25°C ( $\mu\text{mol m}^{-2} \text{s}^{-1}$ )

428 **Figure 2**

429

430 **Figure 2** Effects of CO<sub>2</sub>, nitrogen fertilization, and inoculation on net photosynthesis measured  
 431 at 420 μmol mol<sup>-1</sup> CO<sub>2</sub> (a), net photosynthesis measured under growth CO<sub>2</sub> concentration (b), the  
 432 maximum rate of Rubisco carboxylation at 25°C (c), the maximum rate of electron transport for  
 433 RuBP regeneration at 25°C (d), the ratio of the maximum rate of electron transport for RuBP  
 434 regeneration to the maximum rate of Rubisco carboxylation (e), and dark respiration at 25°C (f).  
 435 Nitrogen fertilization is represented on the x-axis. Red shaded points and trendlines indicate  
 436 plants grown under eCO<sub>2</sub>, while blue shaded points and trendlines indicate plants grown under  
 437 aCO<sub>2</sub>. Light blue and red circular points and trendlines indicate measurements collected from  
 438 uninoculated plants, while dark blue and red triangular points indicate measurements collected  
 439 from inoculated plants. Solid trendlines indicate regression slopes that are different from zero  
 440 ( $p < 0.05$ ), while dashed trendlines indicate slopes that are not distinguishable from zero ( $p > 0.05$ ).

441 *Whole-plant traits*

442 eCO<sub>2</sub> increased total leaf area and total biomass by 51% and 102%, respectively ( $p<0.001$  in  
 443 both cases; Table 3). Positive effects of eCO<sub>2</sub> on total leaf area and total biomass were enhanced  
 444 with increasing nitrogen fertilization (CO<sub>2</sub>-by-nitrogen fertilization interaction:  $p<0.001$  in both  
 445 cases; Table 3; Fig. 4a-b) but not inoculation (CO<sub>2</sub>-by-inoculation interaction:  $p>0.05$  in both  
 446 cases; Table 3). An interaction between nitrogen fertilization and inoculation ( $p<0.001$  in both  
 447 cases; Table 3) indicated that the positive effects of increasing nitrogen fertilization on total leaf  
 448 area and total biomass ( $p<0.001$  in both cases; Table 3) were stronger in uninoculated plants than  
 449 inoculated plants (Tukey tests comparing the nitrogen fertilization-trait slopes between  
 450 inoculation treatments:  $p<0.05$  for both traits).

451 eCO<sub>2</sub> increased  $N_{cost}$  by 62% ( $p<0.001$ ; Table 3), a pattern that was not modified by  
 452 nitrogen fertilization (CO<sub>2</sub>-by-nitrogen fertilization interaction:  $p>0.05$ ; Table 3). An interaction  
 453 between CO<sub>2</sub> and inoculation ( $p<0.05$ ; Table 3) indicated that the positive effect of eCO<sub>2</sub> on  $N_{cost}$   
 454 was stronger in uninoculated plants (99% increase; Tukey test evaluating the CO<sub>2</sub> effect on  $N_{cost}$   
 455 in uninoculated plants:  $p<0.001$ ) than inoculated plants (21% increase Tukey test evaluating the  
 456 CO<sub>2</sub> effect on  $N_{cost}$  in inoculated plants:  $p<0.05$ ). An interaction between nitrogen fertilization  
 457 and inoculation ( $p<0.001$ ; Table 3) indicated that the negative effect of increasing nitrogen  
 458 fertilization on  $N_{cost}$  ( $p<0.001$ ; Table 3) was stronger in uninoculated plants (Tukey test  
 459 comparing the nitrogen fertilization- $N_{cost}$  slope between inoculation treatments:  $p<0.001$ ). A  
 460 three-way interaction ( $p<0.001$ ; Table 3) indicated that interactions between nitrogen fertilization  
 461 and inoculation were stronger under eCO<sub>2</sub> than aCO<sub>2</sub>. This pattern was driven by greater  $N_{cost}$  in  
 462 uninoculated plants grown under eCO<sub>2</sub> and low nitrogen fertilization than any other CO<sub>2</sub>-by-  
 463 inoculation treatment combination under low nitrogen fertilization (Tukey test comparing  $N_{cost}$  in  
 464 uninoculated individuals grown under eCO<sub>2</sub> and 0 ppm N to all other CO<sub>2</sub>-inoculation treatment  
 465 combinations grown under 0 ppm N:  $p<0.001$  in all cases; Fig. 4c).

466

467 *Nitrogen fixation*

468 There was no CO<sub>2</sub> effect on % $N_{dfa}$  ( $p=0.472$ ; Table 3; Fig. 4d). An interaction between nitrogen  
 469 fertilization and inoculation ( $p<0.001$ ; Table 3) indicated that the negative effect of increasing  
 470 nitrogen fertilization on % $N_{dfa}$  ( $p<0.001$ ; Table 3) was driven by inoculated plants (Tukey test of  
 471 the nitrogen fertilization-% $N_{dfa}$  slope in inoculated plants:  $p<0.001$ ), as there was no effect of

472 nitrogen fertilization on  $\%N_{dfa}$  in uninoculated plants (Tukey test of the nitrogen fertilization-  
473  $\%N_{dfa}$  slope in uninoculated plants:  $p>0.05$ ; Fig. 4d).  
474

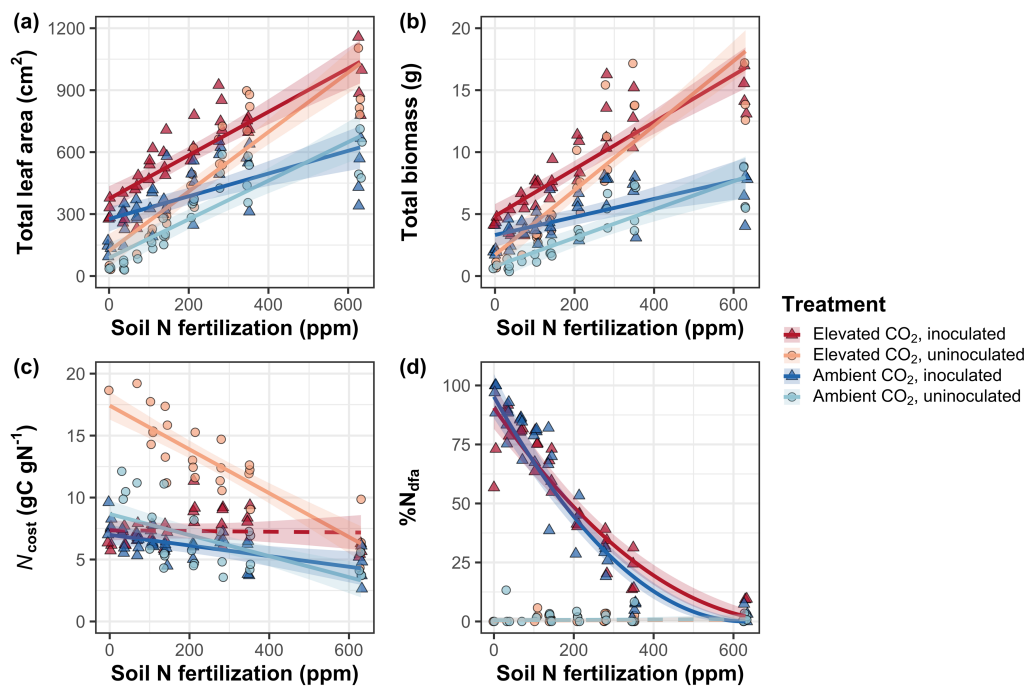
For Peer Review

475 **Table 3** Effects of CO<sub>2</sub> concentration, inoculation, and nitrogen fertilization on whole-plant growth, carbon costs to acquire nitrogen,  
 476 and investment toward symbiotic nitrogen fixation\*

		Total leaf area		Total biomass <sup>b</sup>		Carbon cost to acquire nitrogen		%N <sub>dfa</sub> <sup>b</sup>	
	df	$\chi^2$	p	$\chi^2$	p	$\chi^2$	p	$\chi^2$	p
CO <sub>2</sub>	1	69.291	<0.001	131.477	<0.001	88.189	<0.001	0.518	0.472
Inoculation (I)	1	35.715	<0.001	34.264	<0.001	136.343	<0.001	955.57	<0.001
N fertilization (N)	1	274.199	<0.001	269.046	<0.001	80.501	<0.001	292.938	<0.001
CO <sub>2</sub> *I	1	2.064	0.151	0.518	0.472	85.237	<0.001	2.010	0.156
CO <sub>2</sub> *N	1	18.655	<0.001	16.877	<0.001	1.050	0.306	2.716	0.099
I*N	1	10.804	0.001	15.779	<0.001	46.489	<0.001	231.29	<0.001
CO <sub>2</sub> *I*N	1	<0.001	0.990	0.023	0.880	18.125	<0.001	2.119	0.145

477 \*Significance determined using Type II Wald  $\chi^2$  tests ( $\alpha=0.05$ ). P-values less than 0.05 are in bold. A superscript “<sup>b</sup>” after trait labels  
 478 indicates if models were fit using square root transformed variables. Key: df=degrees of freedom,  $\chi^2$ =Wald chi-square test statistic,  
 479 total leaf area (cm<sup>2</sup>), total biomass (g), carbon cost to acquire nitrogen (gC gN<sup>-1</sup>), %N<sub>dfa</sub>=percent leaf nitrogen content fixed from the  
 480 atmosphere (%).

481

482 **Figure 3**

483

484 **Figure 3.** Effects of CO<sub>2</sub>, nitrogen fertilization, and inoculation on total leaf area (a), total  
 485 biomass (b), structural carbon costs to acquire nitrogen (c), and percent of leaf nitrogen content  
 486 derived from the atmosphere (d). Nitrogen fertilization is represented on the x-axis. Red shaded  
 487 points and trendlines indicate plants grown under eCO<sub>2</sub>, while blue shaded points and trendlines  
 488 indicate plants grown under aCO<sub>2</sub>. Light blue and red circular points and trendlines indicate  
 489 measurements collected from uninoculated plants, while dark blue and red triangular points  
 490 indicate measurements collected from inoculated plants. Solid trendlines indicate regression  
 491 slopes that are different from zero ( $p < 0.05$ ), while dashed trendlines indicate slopes that are not  
 492 distinguishable from zero ( $p > 0.05$ ).  
 493

494 **Discussion**

495 *Glycine max* seedlings were grown under two CO<sub>2</sub> concentrations, two inoculation treatments,  
496 and nine nitrogen fertilization treatments in a full-factorial growth chamber experiment to  
497 reconcile the role of nitrogen availability, demand, and acquisition strategy on leaf and whole-  
498 plant responses to eCO<sub>2</sub>. eCO<sub>2</sub> increased  $A_{\text{net,growth}}$  despite reduced  $N_{\text{area}}$ ,  $V_{\text{cmax25}}$ , and  $J_{\text{max25}}$ .  
499 Larger reductions in  $V_{\text{cmax25}}$  than  $J_{\text{max25}}$  increased  $J_{\text{max25}}:V_{\text{cmax25}}$ , while respective increases and  
500 decreases in  $A_{\text{net,growth}}$  and  $N_{\text{area}}$  increased photosynthetic nitrogen-use efficiency. These patterns  
501 are consistent with previous studies that have investigated or reviewed leaf responses to eCO<sub>2</sub>  
502 (Drake *et al.*, 1997; Ainsworth *et al.*, 2002; Ainsworth & Long, 2005; Ainsworth & Rogers,  
503 2007; Crous *et al.*, 2010; Lee *et al.*, 2011; Smith & Dukes, 2013; Poorter *et al.*, 2022). Positive  
504 effects of eCO<sub>2</sub> on  $A_{\text{net,growth}}$  and  $J_{\text{max25}}:V_{\text{cmax25}}$  and negative effects of eCO<sub>2</sub> on  $V_{\text{cmax25}}$  and  $J_{\text{max25}}$   
505 were not related to nitrogen availability, following patterns expected from eco-evolutionary  
506 optimality theory (Smith & Keenan, 2020; Harrison *et al.*, 2021; Dong *et al.*, 2022b). In further  
507 support of the theory, increased  $J_{\text{max25}}:V_{\text{cmax25}}$  and photosynthetic nitrogen-use efficiency provide  
508 strong support for the idea that leaves were downregulating  $V_{\text{cmax25}}$  in response to eCO<sub>2</sub> such that  
509 enhanced net photosynthesis rates approached optimal coordination of Rubisco carboxylation  
510 and electron transport for RuBP regeneration (Chen *et al.*, 1993; Maire *et al.*, 2012; Smith &  
511 Keenan, 2020), decreasing demand for building and maintaining photosynthetic enzymes (Dong  
512 *et al.*, 2022b).

513 Leaf photosynthetic responses to eCO<sub>2</sub> corresponded with increased total leaf area and  
514 total biomass, patterns that are also consistent with previous studies that have investigated or  
515 reviewed whole-plant responses to eCO<sub>2</sub> (Ainsworth *et al.*, 2002; Ainsworth & Long, 2005;  
516 Smith & Dukes, 2013; Poorter *et al.*, 2022). Greater whole-plant growth under eCO<sub>2</sub> was  
517 associated with greater carbon costs to acquire nitrogen through stronger increases in  
518 belowground carbon allocation than whole-plant nitrogen uptake, indicating that plants grown  
519 under eCO<sub>2</sub> supported greater total leaf area and total biomass through increased plant nitrogen  
520 uptake, though at reduced nitrogen uptake efficiency. Unlike leaf photosynthetic responses,  
521 increasing nitrogen fertilization enhanced positive whole-plant responses to eCO<sub>2</sub>, supporting  
522 our hypothesis that nitrogen availability would constrain whole-plant responses to eCO<sub>2</sub>. Positive  
523 effects of increasing nitrogen fertilization on total leaf area and total biomass were associated  
524 with reductions in carbon costs to acquire nitrogen, a pattern driven by stronger increases in

whole-plant nitrogen uptake than belowground carbon allocation (Perkowski *et al.*, 2021). While reductions in carbon costs to acquire nitrogen due to increasing nitrogen fertilization were similar between CO<sub>2</sub> treatments, increasing nitrogen fertilization increased whole-plant nitrogen uptake more strongly under eCO<sub>2</sub>. This pattern, coupled with similar effects of nitrogen fertilization on belowground carbon allocation responses to eCO<sub>2</sub>, indicated that increasing fertilization enhanced positive growth responses to eCO<sub>2</sub> through increased nitrogen uptake efficiency. These findings support previous results suggesting that positive effects of nitrogen availability on whole-plant responses to eCO<sub>2</sub> are linked to reduced costs of acquiring nitrogen and increased nitrogen uptake efficiency (Terrer *et al.*, 2018).

Nitrogen availability and demand could each explain plant responses to eCO<sub>2</sub>, though these factors operated at different levels of organization. Specifically, eCO<sub>2</sub> increased net photosynthesis rates through increasingly optimal coordination of Rubisco carboxylation and electron transport for RuBP regeneration (Chen *et al.*, 1993; Maire *et al.*, 2012), a pattern that reduced leaf nitrogen demand for building and maintaining photosynthetic enzymes and was independent of changes in nitrogen fertilization. Nitrogen availability enhanced whole-plant responses to eCO<sub>2</sub> despite no apparent effect of nitrogen fertilization at the leaf level. Interestingly, optimized nitrogen allocation to photosynthetic capacity may have resulted in nitrogen savings at the leaf level that could have maximized nitrogen allocation to growth. These results suggest that plants grown under eCO<sub>2</sub> responded to increased nitrogen availability by increasing the number of optimally coordinated leaves and that the downregulation in photosynthetic capacity under eCO<sub>2</sub> was not a direct response to changes in nitrogen availability.

#### *547 Inoculation does not affect leaf or whole-plant responses to eCO<sub>2</sub>*

Inoculation increased  $N_{\text{area}}$ ,  $A_{\text{net},420}$ ,  $A_{\text{net,growth}}$ ,  $V_{\text{cmax}25}$ ,  $J_{\text{max}25}$ , total leaf area, and total biomass, and decreased  $J_{\text{max}25}:V_{\text{cmax}25}$  and  $R_{\text{d}25}$ . These patterns support previous literature suggesting that species that form associations with symbiotic nitrogen-fixing bacteria have increased leaf nitrogen content, photosynthetic capacity, and growth compared to species that do not form such associations (Adams *et al.*, 2016; Bytnerowicz *et al.*, 2023). Positive effects of inoculation on leaf and whole-plant traits were most apparent under low nitrogen fertilization and rapidly diminished with increasing nitrogen fertilization as plant investment in symbiotic nitrogen fixation decreased, supporting the idea that nitrogen fixation is a nutrient acquisition strategy that

556 may confer competitive benefits for nitrogen-fixing species growing in low soil nitrogen  
557 environments (Rastetter *et al.*, 2001; Andrews *et al.*, 2011; McCulloch & Porder, 2021).

558 Interestingly, inoculation did not modify the effect of eCO<sub>2</sub> on  $V_{cmax25}$ ,  $J_{max25}$ ,  
559  $J_{max25}$ : $V_{cmax25}$ , total leaf area, or total biomass. These patterns corresponded with null effects of  
560 eCO<sub>2</sub> on %N<sub>dfa</sub> and the ratio of root nodule biomass to root biomass, suggesting that null  
561 inoculation effects on plant responses to eCO<sub>2</sub> were due to similar plant investments toward  
562 symbiotic nitrogen fixation between CO<sub>2</sub> treatments. We observed these patterns regardless of  
563 nitrogen fertilization level, contrasting our hypothesis that inoculation would enhance whole-  
564 plant responses to eCO<sub>2</sub> under low nitrogen fertilization, where individuals invested more  
565 strongly in symbiotic nitrogen fixation. These patterns also contrast previous work showing that  
566 plant investment toward symbiotic nitrogen fixation tends to be greater under scenarios that  
567 increase whole-plant demand to acquire nitrogen (Taylor & Menge, 2018; Friel & Friesen, 2019;  
568 McCulloch & Porder, 2021; Perkowski *et al.*, 2021). Interestingly, stronger positive effects of  
569 eCO<sub>2</sub> on  $A_{net,growth}$  in inoculated individuals support previously work (Ainsworth *et al.*, 2002).  
570 However, this response was not due to alterations in plant investment toward the symbiosis.  
571

#### 572 *Modeling implications*

573 Many terrestrial biosphere models predict photosynthetic capacity through parameterized  
574 relationships between  $N_{area}$  and  $V_{cmax}$  (Smith & Dukes, 2013; Rogers *et al.*, 2017), which assumes  
575 that leaf nitrogen-photosynthesis relationships are constant across growing environments. Our  
576 results build on previous work suggesting that leaf nitrogen-photosynthesis relationships  
577 dynamically change across growing environments (Luo *et al.*, 2021; Waring *et al.*, 2023), as  
578 eCO<sub>2</sub> reduced leaf nitrogen content more strongly than it increased  $A_{net,growth}$  and decreased  
579  $V_{cmax25}$  and  $J_{max25}$ . Additionally, the positive effect of increasing nitrogen fertilization on indices  
580 of photosynthetic capacity was only apparent in uninoculated plants, as nitrogen fertilization did  
581 not affect  $V_{cmax25}$  or  $J_{max25}$  in inoculated plants. The positive effect of increasing nitrogen  
582 fertilization on  $N_{area}$  and  $Chl_{area}$  was also markedly weaker in inoculated plants than in  
583 uninoculated plants. These patterns indicate that leaf nitrogen-photosynthesis relationships are  
584 context-dependent on nitrogen acquisition strategy, may only be constant in environments where  
585 nitrogen availability limits leaf physiology, and will likely shift in response to increasing  
586 atmospheric CO<sub>2</sub> concentrations. Terrestrial biosphere models that predict photosynthetic

587 capacity through parameterized relationships between  $N_{\text{area}}$  and  $V_{\text{cmax}}$  (Kattge *et al.*, 2009;  
588 Walker *et al.*, 2014) may risk overestimating photosynthetic capacity, therefore net primary  
589 productivity and the magnitude of the land carbon sink, under future novel growth environments.

590 Our results demonstrate that optimal resource allocation to photosynthetic capacity  
591 defines leaf photosynthetic responses to eCO<sub>2</sub> and that these responses are independent of  
592 nitrogen availability. Current approaches for simulating photosynthetic responses to CO<sub>2</sub> in  
593 terrestrial biosphere models with coupled carbon and nitrogen cycles often invoke patterns  
594 expected from progressive nitrogen limitation, where photosynthetic responses to eCO<sub>2</sub> are  
595 modeled as a function of positive relationships between nitrogen availability and leaf nitrogen  
596 content (Smith & Dukes, 2013; Wieder *et al.*, 2015; Rogers *et al.*, 2017). Findings presented here  
597 contradict this framework, suggesting that leaf photosynthetic responses to eCO<sub>2</sub> result in  
598 optimized nitrogen allocation to satisfy reduced leaf nitrogen demand to build and maintain  
599 photosynthetic enzymes. Optimality models that use principles from optimal coordination and  
600 photosynthetic least-cost theories are capable of capturing photosynthetic responses to CO<sub>2</sub>  
601 independent of nitrogen availability (Smith & Keenan, 2020; Harrison *et al.*, 2021), suggesting  
602 that including optimality frameworks in terrestrial biosphere models may improve the accuracy  
603 by which models simulate photosynthetic processes in response to increasing atmospheric CO<sub>2</sub>  
604 concentrations.

605 Previous work has highlighted that pot experiments restrict belowground rooting volume  
606 and may alter plant allocation responses to environmental change (Ainsworth *et al.*, 2002;  
607 Poorter *et al.*, 2012). In this study, the ratio of pot volume to total biomass was greater under  
608 eCO<sub>2</sub> and increased with increasing nitrogen fertilization such that several treatment  
609 combinations exceeded values recommended to avoid growth limitation imposed by pot volume  
610 (<1 g L<sup>-1</sup>; Table S6; Fig. S6) (Poorter *et al.*, 2012). However, there was no evidence to suggest  
611 that pot size limited plant growth, as evidenced by the lack of a saturating effect of increasing  
612 fertilization on total biomass, belowground carbon biomass, or root biomass under conditions  
613 where biomass: pot volume ratios exceeded 1 g L<sup>-1</sup> (e.g., individuals of either inoculation status  
614 grown under high fertilization and eCO<sub>2</sub>). Field studies that do not restrict belowground rooting  
615 volume observed similar leaf and whole-plant responses to eCO<sub>2</sub> (Crous *et al.*, 2010; Lee *et al.*,  
616 2011; Pastore *et al.*, 2019; Smith & Keenan, 2020), indicating that the pot volume used in this  
617 study (6 L) was likely sufficient to avoid growth limitation.

618

619 *Conclusions*

620 Nitrogen availability and demand for building and maintaining photosynthetic enzymes each  
621 helped explain *G. max* responses to eCO<sub>2</sub>, though operated at different scales. Supporting eco-  
622 evolutionary optimality theory, leaf photosynthetic responses to eCO<sub>2</sub> were independent of  
623 nitrogen availability and, in most cases, inoculation. Instead, eCO<sub>2</sub> decreased the maximum rate  
624 of Rubisco carboxylation more strongly than it decreased the maximum rate of electron transport  
625 for RuBP regeneration, allowing increased net photosynthesis rates to approach optimal  
626 coordination while reducing leaf nitrogen demand to build and maintain photosynthetic enzymes.  
627 Supporting the progressive nitrogen limitation hypothesis, nitrogen availability enhanced whole-  
628 plant responses to eCO<sub>2</sub> due to increased plant nitrogen uptake and reduced costs of nitrogen  
629 acquisition. Additionally, cascading effects of nitrogen savings at the leaf level may have  
630 maximized nitrogen allocation to whole-plant growth. Inoculation did not modify whole-plant  
631 responses to eCO<sub>2</sub> due to similar plant investment toward symbiotic nitrogen fixation between  
632 CO<sub>2</sub> treatments. Overall, results indicate that plants grown under eCO<sub>2</sub> responded to increased  
633 nitrogen availability by increasing the number of optimally coordinated leaves, and changes in  
634 nitrogen availability did not modify the downregulation in photosynthetic capacity under eCO<sub>2</sub>.  
635 The differential role of nitrogen availability on leaf and whole-plant responses to eCO<sub>2</sub> coupled  
636 with dynamic leaf nitrogen-photosynthesis relationships across CO<sub>2</sub> and nitrogen fertilization  
637 treatments suggests that terrestrial biosphere models may improve simulations of photosynthetic  
638 responses to increasing atmospheric CO<sub>2</sub> concentrations by adopting frameworks that include  
639 optimality principles.

640

641 **Conflicts of Interest**

642 The authors declare no conflicts of interest.

643

644 **Acknowledgements**

645 This study is a contribution to the LEMONTREE (Land Ecosystem Models based On New  
646 Theory, obseRvations and ExperimEnts) project, funded through the generosity of Eric and  
647 Wendy Schmidt by recommendation of the Schmidt Futures programme. EAP acknowledges  
648 support from a Texas Tech University Doctoral Dissertation Completion Fellowship and a

649 Botanical Society of America Graduate Student Research Award. This work was also supported  
650 by US National Science Foundation awards to NGS (DEB-2045968 and DEB-2217353).

651

## 652 Data Availability

653 All R scripts, data, and metadata are available at <https://doi.org/10.5281/zenodo.10177575> (or on  
654 GitHub at: [https://github.com/eaperkowski/NxCO2xI\\_ms\\_data](https://github.com/eaperkowski/NxCO2xI_ms_data))

655

## 656 Author contributions

657 EAP conceptualized the study objectives and designed the experiment in collaboration with  
658 NGS, collected data, conducted data analysis, and wrote the first manuscript draft. EE assisted  
659 with data collection and experiment maintenance. NGS conceptualized study objectives and  
660 experimental design with EAP and oversaw experiment progress. All authors provided  
661 manuscript feedback and approved the manuscript in its current form for submission to *New  
662 Phytologist*.

663

## 664 References

- 665 **Adams MA, Turnbull TL, Sprent JI, Buchmann N.** 2016. Legumes are different: Leaf  
666 nitrogen, photosynthesis, and water use efficiency. *Proceedings of the National Academy of  
667 Sciences of the United States of America* **113**: 4098–4103.
- 668 **Ainsworth EA, Davey PA, Bernacchi CJ, Dermody OC, Heaton EA, Moore DJ, Morgan  
669 PB, Naidu SL, Ra HSY, Zhu XG, et al.** 2002. A meta-analysis of elevated [CO<sub>2</sub>] effects on  
670 soybean (*Glycine max*) physiology, growth and yield. *Global Change Biology* **8**: 695–709.
- 671 **Ainsworth EA, Long SP.** 2005. What have we learned from 15 years of free-air CO<sub>2</sub> enrichment  
672 (FACE)? A meta-analytic review of the responses of photosynthesis, canopy properties and plant  
673 production to rising CO<sub>2</sub>. *New Phytologist* **165**: 351–372.
- 674 **Ainsworth EA, Rogers A.** 2007. The response of photosynthesis and stomatal conductance to  
675 rising [CO<sub>2</sub>]: mechanisms and environmental interactions. *Plant, Cell & Environment* **30**: 258–  
676 270.
- 677 **Andrews M, James EK, Sprent JI, Boddey RM, Gross E, dos Reis FB.** 2011. Nitrogen  
678 fixation in legumes and actinorhizal plants in natural ecosystems: Values obtained using <sup>15</sup>N  
679 natural abundance. *Plant Ecology and Diversity* **4**: 117–130.

- 680 **Arora VK, Katavouta A, Williams RG, Jones CD, Brovkin V, Friedlingstein P, Schwinger J, Bopp L, Boucher O, Cadule P, et al.** 2020. Carbon-concentration and carbon-climate  
681 feedbacks in CMIP6 models and their comparison to CMIP5 models. *Biogeosciences* **17**: 4173–  
682 4222.
- 683 **Barnes JD, Balaguer L, Manrique E, Elvira S, Davison AW.** 1992. A reappraisal of the use of  
684 DMSO for the extraction and determination of chlorophylls a and b in lichens and higher plants.  
685 *Environmental and Experimental Botany* **32**: 85–100.
- 686 **Bates D, Mächler M, Bolker B, Walker S.** 2015. Fitting linear mixed-effects models using  
687 lme4. *Journal of Statistical Software* **67**: 1–48.
- 688 **Bernacchi CJ, Singsaas EL, Pimentel C, Portis AR, Long SP.** 2001. Improved temperature  
689 response functions for models of Rubisco-limited photosynthesis. *Plant, Cell and Environment*  
690 **24**: 253–259.
- 691 **Brzostek ER, Fisher JB, Phillips RP.** 2014. Modeling the carbon cost of plant nitrogen  
692 acquisition: Mycorrhizal trade-offs and multipath resistance uptake improve predictions of  
693 retranslocation. *Journal of Geophysical Research: Biogeosciences* **119**: 1684–1697.
- 694 **Bytnerowicz TA, Funk JL, Menge DNL, Perakis SS, Wolf AA.** 2023. Leaf nitrogen affects  
695 photosynthesis and water use efficiency similarly in nitrogen-fixing and non-fixing trees. *Journal  
696 of Ecology*: 1–15.
- 697 **Chen J-L, Reynolds JF, Harley PC, Tenhunen JD.** 1993. Coordination theory of leaf nitrogen  
698 distribution in a canopy. *Oecologia* **93**: 63–69.
- 699 **Crous KY, Reich PB, Hunter MD, Ellsworth DS.** 2010. Maintenance of leaf N controls the  
700 photosynthetic CO<sub>2</sub> response of grassland species exposed to 9 years of free-air CO<sub>2</sub> enrichment.  
701 *Global Change Biology* **16**: 2076–2088.
- 702 **Curtis PS.** 1996. A meta-analysis of leaf gas exchange and nitrogen in trees grown under  
703 elevated carbon dioxide. *Plant, Cell and Environment* **19**: 127–137.
- 704 **Davies-Barnard T, Meyerholt J, Zaeble S, Friedlingstein P, Brovkin V, Fan Y, Fisher RA,  
705 Jones CD, Lee H, Peano D, et al.** 2020. Nitrogen cycling in CMIP6 land surface models:  
706 progress and limitations. *Biogeosciences* **17**: 5129–5148.
- 707 **Dong N, Prentice IC, Evans BJ, Caddy-Retalic S, Lowe AJ, Wright IJ.** 2017. Leaf nitrogen  
708 from first principles: field evidence for adaptive variation with climate. *Biogeosciences* **14**: 481–  
709 495.

- 711 **Dong N, Prentice IC, Wright IJ, Evans BJ, Togashi HF, Caddy-Retalic S, McInerney FA,**  
712 **Sparrow B, Leitch E, Lowe AJ.** 2020. Components of leaf-trait variation along environmental  
713 gradients. *New Phytologist* **228**: 82–94.
- 714 **Dong N, Prentice IC, Wright IJ, Wang H, Atkin OK, Bloomfield KJ, Domingues TF,**  
715 **Gleason SM, Maire V, Onoda Y, et al.** 2022a. Leaf nitrogen from the perspective of optimal  
716 plant function. *Journal of Ecology* **110**: 2585–2602.
- 717 **Dong N, Wright IJ, Chen JM, Luo X, Wang H, Keenan TF, Smith NG, Prentice IC.** 2022b.  
718 Rising CO<sub>2</sub> and warming reduce global canopy demand for nitrogen. *New Phytologist* **235**:  
719 1692–1700.
- 720 **Drake BG, González-Meler MA, Long SP.** 1997. More efficient plants: a consequence of  
721 rising atmospheric CO<sub>2</sub>? *Annual Review of Plant Biology* **48**: 609–639.
- 722 **Duursma RA.** 2015. Plantcophys - an R package for analysing and modelling leaf gas  
723 exchange data. *PLOS ONE* **10**: e0143346.
- 724 **Evans JR.** 1989. Photosynthesis and nitrogen relationships in leaves of C<sub>3</sub> plants. *Oecologia* **78**:  
725 9–19.
- 726 **Evans JR, Clarke VC.** 2019. The nitrogen cost of photosynthesis. *Journal of Experimental*  
727 *Botany* **70**: 7–15.
- 728 **Farquhar GD, von Caemmerer S, Berry JA.** 1980. A biochemical model of photosynthetic  
729 CO<sub>2</sub> assimilation in leaves of C<sub>3</sub> species. *Planta* **149**: 78–90.
- 730 **Field CB, Mooney HA.** 1986. The photosynthesis-nitrogen relationship in wild plants. In:  
731 Givnish TJ, ed. *On the Economy of Plant Form and Function*. Cambridge: Cambridge University  
732 Press, 25–55.
- 733 **Finzi AC, Moore DJP, DeLucia EH, Lichter J, Hofmockel KS, Jackson RB, Kim HS,**  
734 **Matamala R, McCarthy HR, Oren R, et al.** 2006. Progressive nitrogen limitation of ecosystem  
735 processes under elevated CO<sub>2</sub> in a warm-temperate forest. *Ecology* **87**: 15–25.
- 736 **Fox J, Weisberg S.** 2019. *An R companion to applied regression*. Thousand Oaks, California:  
737 Sage.
- 738 **Friedlingstein P, Meinshausen M, Arora VK, Jones CD, Anav A, Liddicoat SK, Knutti R.**  
739 **2014.** Uncertainties in CMIP5 climate projections due to carbon cycle feedbacks. *Journal of*  
740 *Climate* **27**: 511–526.

- 741 **Friel CA, Friesen ML.** 2019. Legumes modulate allocation to rhizobial nitrogen fixation in  
742 response to factorial light and nitrogen manipulation. *Frontiers in Plant Science* **10**: 1316.
- 743 **Harrison SP, Cramer W, Franklin O, Prentice IC, Wang H, Bränström Å, de Boer H,**  
744 **Dieckmann U, Joshi J, Keenan TF, et al.** 2021. Eco-evolutionary optimality as a means to  
745 improve vegetation and land-surface models. *New Phytologist* **231**: 2125–2141.
- 746 **Hoagland DR, Arnon DI.** 1950. The water-culture method for growing plants without soil.  
747 *California Agricultural Experiment Station*: 347 **347**: 1–32.
- 748 **Hungate BA, Dukes JS, Shaw MR, Luo Y, Field CB.** 2003. Nitrogen and climate change.  
749 *Science* **302**: 1512–1513.
- 750 **Katabuchi M.** 2015. LeafArea: An R package for rapid digital analysis of leaf area. *Ecological*  
751 *Research* **30**: 1073–1077.
- 752 **Kattge J, Knorr W, Raddatz T, Wirth C.** 2009. Quantifying photosynthetic capacity and its  
753 relationship to leaf nitrogen content for global-scale terrestrial biosphere models. *Global Change*  
754 *Biology* **15**: 976–991.
- 755 **Kenward MG, Roger JH.** 1997. Small sample inference for fixed effects from restricted  
756 maximum likelihood. *Biometrics* **53**: 983.
- 757 **Kou-Giesbrecht S, Arora VK, Seiler C, Arneth A, Falk S, Jain AK, Joos F, Kennedy D,**  
758 **Knauer J, Sitch S, et al.** 2023. Evaluating nitrogen cycling in terrestrial biosphere models: a  
759 disconnect between the carbon and nitrogen cycles. *Earth System Dynamics* **14**: 767–795.
- 760 **LeBauer DS, Treseder K.** 2008. Nitrogen limitation of net primary productivity. *Ecology* **89**:  
761 371–379.
- 762 **Lee TD, Barrott SH, Reich PB.** 2011. Photosynthetic responses of 13 grassland species across  
763 11 years of free-air CO<sub>2</sub> enrichment is modest, consistent and independent of N supply. *Global*  
764 *Change Biology* **17**: 2893–2904.
- 765 **Lenth R.** 2019. emmeans: estimated marginal means, aka least-squares means.
- 766 **Liang J, Qi X, Souza L, Luo Y.** 2016. Processes regulating progressive nitrogen limitation  
767 under elevated carbon dioxide: a meta-analysis. *Biogeosciences* **13**: 2689–2699.
- 768 **Luo Y, Currie WS, Dukes JS, Finzi AC, Hartwig UA, Hungate BA, McMurtrie RE, Oren**  
769 **R, Parton WJ, Pataki DE, et al.** 2004. Progressive nitrogen limitation of ecosystem responses  
770 to rising atmospheric carbon dioxide. *BioScience* **54**: 731–739.

- 771 **Luo X, Keenan TF, Chen JM, Croft H, Prentice IC, Smith NG, Walker AP, Wang H, Wang**  
772 **R, Xu C, et al.** 2021. Global variation in the fraction of leaf nitrogen allocated to photosynthesis.  
773 *Nature Communications* **12**: 4866.
- 774 **Maire V, Martre P, Kattge J, Gastal F, Esser G, Fontaine S, Soussana J-F.** 2012. The  
775 coordination of leaf photosynthesis links C and N fluxes in C<sub>3</sub> plant species. *PLoS ONE* **7**:  
776 e38345.
- 777 **McCulloch LA, Porder S.** 2021. Light fuels while nitrogen suppresses symbiotic nitrogen  
778 fixation hotspots in neotropical canopy gap seedlings. *New Phytologist* **231**: 1734–1745.
- 779 **Meyerholt J, Sickel K, Zaehle S.** 2020. Ensemble projections elucidate effects of uncertainty in  
780 terrestrial nitrogen limitation on future carbon uptake. *Global Change Biology* **26**: 3978–3996.
- 781 **Moore DJP, Aref S, Ho RM, Pippen JS, Hamilton JG, De Lucia EH.** 2006. Annual basal area  
782 increment and growth duration of *Pinus taeda* in response to eight years of free-air carbon  
783 dioxide enrichment. *Global Change Biology* **12**: 1367–1377.
- 784 **Norby RJ, Warren JM, Iversen CM, Medlyn BE, McMurtrie RE.** 2010. CO<sub>2</sub> enhancement  
785 of forest productivity constrained by limited nitrogen availability. *Proceedings of the National  
786 Academy of Sciences* **107**: 19368–19373.
- 787 **Paillassa J, Wright IJ, Prentice IC, Pepin S, Smith NG, Ethier G, Westerband AC,**  
788 **Lamarque LJ, Wang H, Cornwell WK, et al.** 2020. When and where soil is important to  
789 modify the carbon and water economy of leaves. *New Phytologist* **228**: 121–135.
- 790 **Pastore MA, Lee TD, Hobbie SE, Reich PB.** 2019. Strong photosynthetic acclimation and  
791 enhanced water-use efficiency in grassland functional groups persist over 21 years of CO<sub>2</sub>  
792 enrichment, independent of nitrogen supply. *Global Change Biology* **25**: 3031–3044.
- 793 **Peng Y, Bloomfield KJ, Cernusak LA, Domingues TF, Prentice IC.** 2021. Global climate and  
794 nutrient controls of photosynthetic capacity. *Communications Biology* **4**: 462.
- 795 **Perkowski EA, Waring EF, Smith NG.** 2021. Root mass carbon costs to acquire nitrogen are  
796 determined by nitrogen and light availability in two species with different nitrogen acquisition  
797 strategies. *Journal of Experimental Botany* **72**: 5766–5776.
- 798 **Poorter H, Böhler J, Van Dusschoten D, Climent J, Postma JA.** 2012. Pot size matters: A  
799 meta-analysis of the effects of rooting volume on plant growth. *Functional Plant Biology* **39**:  
800 839–850.

- 801 **Poorter H, Knopf O, Wright IJ, Temme AA, Hogewoning SW, Graf A, Cernusak LA, Pons**  
802 **TL. 2022.** A meta-analysis of responses of C<sub>3</sub> plants to atmospheric CO<sub>2</sub>: dose–response curves  
803 for 85 traits ranging from the molecular to the whole-plant level. *New Phytologist* **233**: 1560–  
804 1596.
- 805 **Prentice IC, Dong N, Gleason SM, Maire V, Wright IJ. 2014.** Balancing the costs of carbon  
806 gain and water transport: testing a new theoretical framework for plant functional ecology.  
807 *Ecology Letters* **17**: 82–91.
- 808 **Prentice IC, Liang X, Medlyn BE, Wang Y-P. 2015.** Reliable, robust and realistic: The three  
809 R's of next-generation land-surface modelling. *Atmospheric Chemistry and Physics* **15**: 5987–  
810 6005.
- 811 **R Core Team. 2021.** R: A language and environment for statistical computing.
- 812 **Rastetter EB, Vitousek PM, Field CB, Shaver GR, Herbert D, Ågren GI. 2001.** Resource  
813 optimization and symbiotic nitrogen fixation. *Ecosystems* **4**: 369–388.
- 814 **Reich PB, Hobbie SE, Lee T, Ellsworth DS, West JB, Tilman D, Knops JMH, Naeem S,**  
815 **Trost J. 2006.** Nitrogen limitation constrains sustainability of ecosystem response to CO<sub>2</sub>.  
816 *Nature* **440**: 922–925.
- 817 **Rogers A, Medlyn BE, Dukes JS, Bonan GB, Caemmerer S, Dietze MC, Kattge J, Leakey**  
818 **ADB, Mercado LM, Niinemets Ü, et al. 2017.** A roadmap for improving the representation of  
819 photosynthesis in Earth system models. *New Phytologist* **213**: 22–42.
- 820 **Saathoff AJ, Welles J. 2021.** Gas exchange measurements in the unsteady state. *Plant Cell and*  
821 *Environment* **44**: 3509–3523.
- 822 **Schneider CA, Rasband WS, Eliceiri KW. 2012.** NIH Image to ImageJ: 25 years of image  
823 analysis. *Nature Methods* **9**: 671–675.
- 824 **Smith NG, Dukes JS. 2013.** Plant respiration and photosynthesis in global-scale models:  
825 incorporating acclimation to temperature and CO<sub>2</sub>. *Global Change Biology* **19**: 45–63.
- 826 **Smith NG, Keenan TF. 2020.** Mechanisms underlying leaf photosynthetic acclimation to  
827 warming and elevated CO<sub>2</sub> as inferred from least-cost optimality theory. *Global Change Biology*  
828 **26**: 5202–5216.
- 829 **Smith NG, Keenan TF, Prentice IC, Wang H, Wright IJ, Niinemets Ü, Crous KY,**  
830 **Domingues TF, Guerrieri R, Ishida FY, et al. 2019.** Global photosynthetic capacity is  
831 optimized to the environment. *Ecology Letters* **22**: 506–517.

- 832 **Taylor BN, Menge DNL.** 2018. Light regulates tropical symbiotic nitrogen fixation more  
833 strongly than soil nitrogen. *Nature Plants* **4**: 655–661.
- 834 **Terrer C, Vicca S, Stocker BD, Hungate BA, Phillips RP, Reich PB, Finzi AC, Prentice IC.**  
835 2018. Ecosystem responses to elevated CO<sub>2</sub> governed by plant–soil interactions and the cost of  
836 nitrogen acquisition. *New Phytologist* **217**: 507–522.
- 837 **Walker AP, Beckerman AP, Gu L, Kattge J, Cernusak LA, Domingues TF, Scales JC,**  
838 **Wohlfahrt G, Wullschleger SD, Woodward FI.** 2014. The relationship of leaf photosynthetic  
839 traits - V<sub>cmax</sub> and J<sub>max</sub> - to leaf nitrogen, leaf phosphorus, and specific leaf area: a meta-analysis  
840 and modeling study. *Ecology and Evolution* **4**: 3218–3235.
- 841 **Wang H, Prentice IC, Keenan TF, Davis TW, Wright IJ, Cornwell WK, Evans BJ, Peng C.**  
842 2017. Towards a universal model for carbon dioxide uptake by plants. *Nature Plants* **3**: 734–741.
- 843 **Waring EF, Perkowski EA, Smith NG.** 2023. Soil nitrogen fertilization reduces relative leaf  
844 nitrogen allocation to photosynthesis. *Journal of Experimental Botany* **74**: 5166–5180.
- 845 **Wellburn AR.** 1994. The spectral determination of chlorophylls a and b, as well as total  
846 carotenoids, using various solvents with spectrophotometers of different resolution. *Journal of*  
847 *Plant Physiology* **144**: 307–313.
- 848 **Wieder WR, Cleveland CC, Smith WK, Todd-Brown K.** 2015. Future productivity and  
849 carbon storage limited by terrestrial nutrient availability. *Nature Geoscience* **8**: 441–444.
- 850 **Wright IJ, Reich PB, Westoby M.** 2003. Least-cost input mixtures of water and nitrogen for  
851 photosynthesis. *The American Naturalist* **161**: 98–111.
- 852